

**Ion-irradiation-induced welding of carbon nanotubes**

A. V. Krasheninnikov, K. Nordlund, and J. Keinonen

*Accelerator Laboratory, P.O. Box 43, FIN-00014 University of Helsinki, Finland*

F. Banhart

*Z.E. Elektronenmikroskopie, Universität Ulm, 89069 Ulm, Germany*

(Received 20 June 2002; revised manuscript received 19 August 2002; published 4 December 2002)

As recent transmission electron microscopy experiments demonstrate, electron irradiation can be used to create molecular junctions between carbon nanotubes. Employing empirical potential molecular dynamics, we study ion bombardment of crossed nanotubes as an alternative technique to join nanotubes. We demonstrate that ion irradiation should result in welding of crossed nanotubes, both suspended and deposited on substrates. We further discuss various experimental aspects of this method which may potentially be used for developing complicated networks of joined nanotubes.

DOI: 10.1103/PhysRevB.66.245403

PACS number(s): 81.07.De, 61.80.Jh, 61.80.Az

**I. INTRODUCTION**

The problem of connecting carbon nanotubes has recently generated considerable interest<sup>1–17</sup> because of the possibility for joined nanotubes to be the building blocks of various nanoscale electronic devices.<sup>3</sup> In particular, two-terminal heterostructures have been shown to work as quantum dots<sup>4,5</sup> or diodes,<sup>6,7</sup> and multiterminal heterostructures (“Y” and “T” nanotube junctions) as nanoscale transistor devices.<sup>8,10</sup>

The two-terminal heterostructures can conceptually be formed by joining single-walled carbon nanotubes (SWNT’s) with different chiralities end-to-end via the introduction of pentagon-heptagon defects<sup>3,4,18</sup> at the interface of the nanotubes. This can also result in the formation of sharp kinks at the joints.<sup>3</sup> Electronic transport and scanning probe microscopy (SPM) experiments<sup>7,19</sup> provide evidence that such kinks indeed exist and appear at the joints of nanotubes with different diameters and chiralities. Thus, it is in principle possible to join nanotubes at their ends. However, these experiments were carried out on nanotubes in which kinks had already been present. It is not quite clear yet how nanotubes of predetermined lengths and chiralities can experimentally be joined.

As for experimental realizations of multiterminal heterostructures, a high-yield fabrication of multiwalled nanotubes with Y junctions has been reported.<sup>8–13</sup> The diameters of the nanotube in the “stem” and “branch” parts of the “Y” junction were adjustable, which potentially opens up a way of producing devices with desired characteristics. Unfortunately, this technique does not allow one to make a more complicated network of joint nanotubes with predetermined positions of junctions between nanotubes.

Interconnections between nanotubes have also been made by chemical functionalization<sup>14</sup> or by nanotube soldering.<sup>15</sup> The latter has been done in a scanning electron microscope by scanning a beam of 1 nm in diameter over a rectangular area with an edge length of tens of nanometers, which resulted in a carbon contamination deposition selectively at nanotube junctions.

It has also been suggested<sup>16</sup> to use a low-energy (3 eV) bombardment of crossed nanotubes with carbon ions to form

carbon chains between the nanotubes and, thus, to solder them. However, the mechanical stability of these junctions and the control over the electrical properties of such hetero-systems is still an open question.

A fundamentally different approach to make connections between nanotubes was recently put forward.<sup>17</sup> It was demonstrated that crossed SWNT’s can be welded together by irradiating the junction in a transmission electron microscope (TEM). The junctions were created due to defects (vacancies and interstitials) induced by a high energy (1.25 MeV) focused electron beam. The annealing of defects via interstitial atom migration and dangling bond saturation gave rise to the formation of intertube covalent bonds and eventually to the Y, X, and T junctions.

In this work, making use of molecular dynamics with empirical potentials, we theoretically study ion irradiation of nanotubes as a technique for forming nanotube junctions. We suggest the utilization of ion irradiation and crossed SWNTs to create multiterminal nanotube heterostructures. We consider suspended (free-standing) crossed nanotubes and nanotubes on atomically flat substrates (supported nanotubes). The latter can be developed by, e.g., deposition from a nanotube dispersion in dichloroethane<sup>20</sup> or by atom force microscope (AFM) manipulation.<sup>21</sup> We demonstrate that ion irradiation combined with high-temperature annealing can be used to weld nanotubes together. We also show that in the absence of irradiation, even with a force pushing crossed nanotubes towards each other and at high temperatures, the nanotube welding does not occur. We finally predict optimum ion doses and energies for the ion-mediated nanotube welding.

**II. COMPUTATIONAL DETAILS**

Our simulation method has been described at length in our previous publications.<sup>22–24</sup> We give here only a brief description of the computational technique used and stress the details important for the simulations.

We used classical molecular dynamics<sup>25</sup> to model the defect production under argon ion irradiation in a system composed of crossed nanotubes. This is the only method fast

enough for realistic atomistic simulations of energetic collisional processes in relatively large systems composed of thousands of atoms. To model covalent carbon-carbon interaction, we used the Brenner II interatomic potential.<sup>26</sup> This potential has been used for simulating carbon nanotubes, and a good correlation between the results of classical simulations and *ab initio* calculations has been reported.<sup>27,28</sup> Because the bond conjugation is not significant in the collisional processes,<sup>22</sup> we neglected the computationally intensive four-body part of the potential in the ion impact simulations. To describe van der Waals interaction between carbon atoms in different nanotubes, we employed a potential<sup>24</sup> which has been developed earlier by us for simulating the interlayer interaction in graphite. We stress, however, that the intertube van der Waals interaction is essential only between *pristine* nanotubes where all the carbon atoms are in the  $sp^2$  hybridization. When covalent bonds between nanotubes have been formed, the energetics of the system is governed by these covalent bonds, but not by van der Waals interaction which is much weaker for nanotubes with diameters less than 20 Å.

To realistically model energetic collisions, we smoothly joined a repulsive potential calculated by a density-functional theory method<sup>29</sup> to the potentials for carbon at short interatomic separations. The joining to the equilibrium potential was done using a Fermi function, with the parameters given in Ref. 24. The interaction between Ar and C was modeled with the Ziegler-Biersack-Littmark universal repulsive potential.<sup>30</sup>

We used open boundary conditions. To prevent spurious reflections of pressure waves from the borders of the system, the Berendsen temperature control<sup>31</sup> was used at the borders for the first 10 ps after the ion impact. Similar to experiments on the electron irradiation<sup>15</sup> of crossed carbon nanotubes, the system temperature was chosen to be 1000 K. In order to estimate the defect annealing during macroscopic times between ion impacts onto a system of about 100 nm<sup>2</sup> (time intervals between ion impacts are longer than microsecond even for the highest irradiation currents experimentally attainable), we simulated the system evolution over 100 ps at 2000 K. After that the temperature was scaled down to the irradiation temperature (1000 K) at a rate of 10 K/ps. This computational technique made it possible to gain insight into the behavior of defects on macroscopic time scales.

The annealing of defects between ion impacts can be also effectively modeled with Monte Carlo techniques. However, it requires knowing all important defect migration rates and mechanisms, as well as reactions between different defect configurations. For example, to simulate one of the annealing mechanisms—migration of carbon adatoms over nanotube surface followed by vacancy-adatom recombination—we have to know the migration path, the corresponding activation energies and prefactors, and the recombination mechanism. Studies on determining the most probable defect annealing channels and estimating the corresponding rates are underway.

We considered crossed 100 Å-long SWNTs of different chiralities and diameters implying that they are fragments of much longer nanotubes. In our simulations, we assumed that

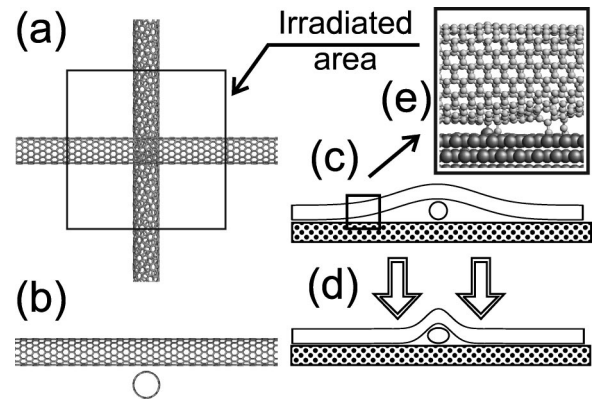


FIG. 1. Schematic illustration of the theoretical setup used for simulations of crossed nanotube welding under ion irradiation. Top (a) and side (b) view of two suspended crossed nanotubes. Crossed nanotubes on a substrate before ion bombardment (c). Development of the force exerted by the upper tube on the lower one due to the irradiation-induced pinning of the nanotubes to the substrate (d). Ball-and-stick representation of a nanotube-substrate interface with the irradiation-induced bonds (e).

the theoretical setup corresponds to either suspended (free standing) crossed nanotubes or those lying on a substrate; see Fig. 1.

The first situation has been studied by Terrones *et al.*<sup>17</sup> for the case of electron irradiation. The crossed nanotubes were deposited on the specimen grid of a TEM and did not interact with the environment near the crossing point.

For the suspended nanotubes, we kept the nanotube ends fixed during ion impact simulations, but during the annealing all the atoms were allowed to move. Because we were interested in irradiation-induced phenomena near the tube contact, we irradiated only the junction area, as shown in Fig. 1(a).

However, for supported nanotubes, the presence of the substrate is quite important, since ion irradiation results in irradiation-induced pinning of nanotubes to the substrate<sup>23</sup> and, hence, in some extra force exerted by the upper SWNT on the lower one, as schematically illustrated in Fig. 1(d).

Because of computational limitations, we were not able to account explicitly for this irradiation-stimulated nanotube-substrate interaction. To adequately describe mechanical deformation of carbon network in crossed pristine nanotubes, their length should be at least 500 Å (i.e., about 10<sup>4</sup> carbon atoms in the simulation cell). Given that carbon potentials are computationally quite expensive and that the number of atoms in the substrate should be one order of magnitude higher, this practically prevents us from achieving a comprehensive statistics in ion impact simulations over a realistic time. However, we simulated ion irradiation of a (10,10) SWNT on a platinum substrate and found that, indeed, if one end of the nanotube is elevated, the irradiation leads to pressing the nanotube due to formations of irradiation-induced covalent bonds, as shown in Fig. 1(e). In order to account for this pressing, we moved down the boundary atoms at the ends of the upper nanotube by 0.05 Å after every ion impact (before running the annealing simulations). Typical values of the irradiation-induced force were in the range 10–40 nN

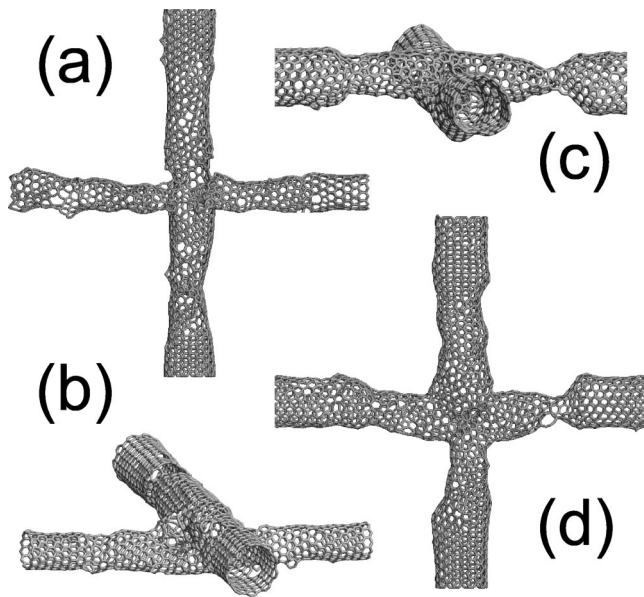


FIG. 2. Molecular models of irradiated crossed carbon nanotubes in the stick representation. Top (a) and side (b) view of the interface of suspended (10,10) and (12,0) nanotubes. Side (c) and top (d) view of the interface of supported (10,10) and (10,10) nanotubes.

(the actual value depends on tube diameters, defect distribution, and other factors).

As for the extra damage in nanotubes created by the sputtered substrate atoms, this damage can anneal quite easily<sup>23</sup> provided that ion energy is not too high (less than 1 keV). The reason behind this fact is that backward sputtered substrate and carbon atoms are much less energetic than the incident Ar ion and create mostly close Frenkel pairs (for SWNT, a vacancy and carbon adatom adsorbed onto the nanotube wall) which anneal due to adatom migration.

### III. RESULTS AND ANALYSIS

To explore the potentialities of using ion irradiation for nanotube welding, we address the following issues: (i) Is ion-irradiation induced welding of SWNT's in principle possible? (ii) What is the optimum energy range of incident ions? (iii) What is the optimum irradiation dose?

We carried out simulations of Ar ion bombardment of crossed SWNTs characterized by the chiral indices as follow: (10,10)-(10,10); (12,0)-(10,10); (12,0)-(10,3); (16,0)-(16,0). Although the choice of the nanotube chirality was somewhat arbitrary, the expectation is that the simulation results are qualitatively correct for SWNT's with diameters in a range of from 8 to 20 Å and weakly depend on the chiralities of crossed nanotubes. For every pair of nanotubes, we irradiated the system with Ar ions having energies  $E_i=0.4, 0.8,$  and 1 keV.

Typical atomic configurations of crossed nanotubes with various chiralities after ion bombardment are shown in Fig. 2. A molecular model for (10,10)-(12,0) suspended crossed SWNT's is presented in Figs. 2(a) and 2(b) with the irradiation dose  $\Phi=0.5\times 10^{15}$  cm<sup>-2</sup>. Figures 2(c) and 2(d) show

the interface of (10,10)-(10,10) supported crossed SWNT's,  $\Phi=0.9\times 10^{15}$  cm<sup>-2</sup>. Only the central part of the system was irradiated, as described above. It is seen that covalent bonds between nanotubes have been formed during the irradiation. These bonds appeared near irradiation-induced defects, mostly vacancies, due to the dangling bond saturation. Formations of these bonds always resulted in lowering the total potential energy of the system with defects, when a number of carbon atoms have been removed by incident ions from the interface region.

For the nanotubes on a substrate, the extra pressure at the crossing point originating from the nanotube-substrate interaction resulted in almost complete merging of nanotubes at the crossing point. The suspended SWNT's were soldered together rather than welded by forming the real X junction. We stress, however, that the experimentally observed merging of nanotubes under electron irradiation<sup>17</sup> occurs at high temperatures on time scales of minutes, similar to irradiation-mediated nanotube coalescence<sup>32</sup> or transformation of carbon onions to diamond.<sup>33,34</sup> This time scale cannot be achieved in present-day atomistic simulations due to computational limitations. Thus, these atomic configurations should be considered as intermediate states, which, nevertheless, outline the route to the complete merging of nanotubes by forming an interface between two nanotubes consisting only of hexagon and pentagon rings.

The bombardment also resulted in sputtering of a substantial amount of atoms from the nanotubes, amorphization of the atomic networks, and the shrinkage of the apparent nanotube diameter. This reduction in the nanotube diameter is due to the healing of irradiation-induced vacancies through dangling bond saturation. A similar behavior of nanotubes under electron irradiation has been reported by Ajayan *et al.*<sup>35</sup> Note that at the irradiation doses used in our simulations, the SWNT's preserved tubular form and remained hollow.

In spite of defect annealing between ion impacts at elevated temperatures, a large number of defects are clearly evident in the nanotube network. One can expect that a substantial amount of defects would anneal in experiments due to the migration<sup>36</sup> of carbon interstitial (adatoms on nanotube walls). However, because of the mentioned above limitations on the simulation time, this did not take place in our simulations. It should also be emphasized that the empirical potential approach tends to overestimate the migration barriers for defects in nanotubes.<sup>37</sup> The irradiation-induced defect should disappear to a large extent after macroscopically long high-temperature annealing. Thus, although ion bombardment creates damage not only in the junction area but also far from it, ion irradiation of nanotubes combined with high-temperature treatment can be used to weld nanotubes together and preserve, at the same time, their tubular form.

We found that the irradiation-induced welding occurs for nanotubes having any chirality, although the mechanical stability and the welding time should depend on the chirality because of the different number of pentagons needed to join the networks of nanotubes with different chiralities.

Having demonstrated a possibility for nanotube welding with the help of an ion beam, we proceed to the issue of the optimum range of ion energies. If ion energies are too low,

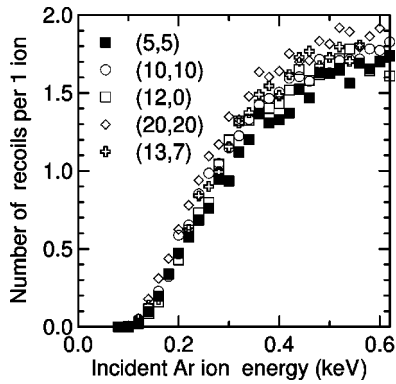


FIG. 3. Number of energetic recoils (both Ar and C atoms) created by an ion impact on the upper crossed nanotube near the junction area as a function of incident ion energy. These recoils hit the lower nanotube creating defects in it, which eventually results in the formation of inter-tube covalent bonds.

very few defects in the interface region will be formed. On the other hand, highly energetic ions will give rise to formations of severely damaged regions (or to a complete breakup of a nanotube), especially for nanotubes on substrates. For supported nanotubes, high energy ions will inevitably result in sputtering of a substantial number of energetic substrate atoms, which will pose considerable problems for the damage control.

One can expect that the criterion for the optimum energy of an Ar ion is that the incident ion should be energetic enough to penetrate through the upper nanotube and displace one or two carbon atoms of the lower nanotube. Carbon atoms can be knocked off from the lower nanotube by not only Ar ions, but also carbon recoils.

We simulated impact events of Ar ions with energies  $E_i$  from 0.1 keV up to 0.6 keV on SWNT's with various chiralities. The impact points were randomly chosen over the upper SWNT surface in the junction area. For every ion energy considered, we carried out 400 independent runs and averaged the results.

In Fig. 3 we plot the number of energetic recoils (both Ar and C atoms) which can damage the lower nanotube as a function of  $E_i$ . Since an Ar ion should have an energy of at least 34 eV to displace a carbon atom from a graphitic network (and roughly the same energy for a carbon recoil<sup>38</sup>), by an energetic recoil we imply an atom/ion with a kinetic energy higher than 34 eV. It is evident from Fig. 3 that energetic recoils below a SWNT appear at a certain ion energy  $E_{th} \approx 0.1$  keV, which is independent of the nanotube chirality. The number of recoils grows up quickly with  $E_i$  up to  $E_i \approx 0.5$  keV, then it slightly depends on  $E_i$ . Such a behavior correlates with the damage production in SWNT's under Ar ion irradiation<sup>23</sup> which saturates at  $E_i \geq 0.6$  keV.

The average energy of the recoils is plotted against  $E_i$  in Fig. 4. We stress once more that we take into consideration the recoils with energies higher than 34 eV. The average recoil energy increases with  $E_i$  and is independent of the nanotube chirality.

As mentioned above, in the impact simulation we neglected the computationally intensive four-body part of the

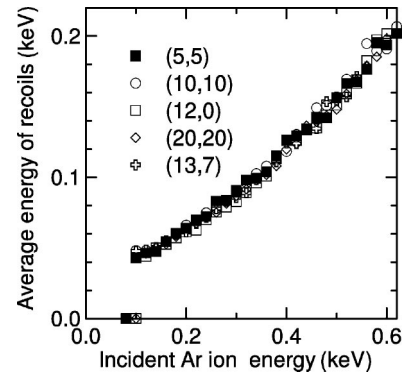


FIG. 4. Average energy of energetic recoils (both Ar and C atoms) as a function of incident ion energy.

Brenner potential. Control runs with the full potential gave essentially the same results (the average energy of the energetic recoils was the same within the statistical error and the number of energetic recoils was about 5 percent lower).

Given that the number of energetic recoils below the upper nanotube should not be too small (a very high irradiation dose is needed in this case for welding) and, on the other hand,  $E_i$  should not be too high (to avoid severe local damage and atoms sputtered from the substrate), we can conclude from Figs. 3 and 4 that the optimum ion energy should be in a range of 0.4–0.6 keV.

The next parameter to be addressed is the optimum irradiation dose. Even if the energy of incident ions is right, an excessive irradiation dose will result in a total destruction of irradiated nanotubes. In Figs. 5(a,b) we present examples of highly damaged crossed nanotubes after an irradiation dose  $\Phi = 2 \times 10^{15} \text{ cm}^{-2}$ . It is seen that this irradiation dose gave rise to the breakup of nanotubes, strong amorphization, and partial loss of the tubular shape. Irradiation of crossed nanotubes with various chiralities gave qualitatively similar results, although we found that the maximum permissible irra-

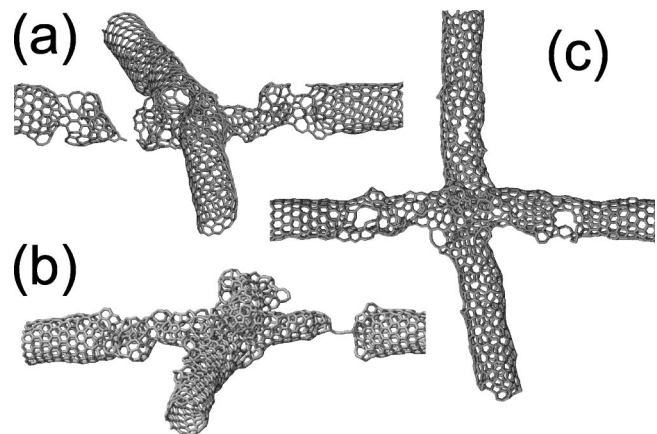


FIG. 5. Molecular models of crossed carbon nanotubes in the stick representation after a high-dose irradiation. Examples of a breakup of nanotubes (a) and strong amorphization of the carbon network (b) when the irradiation dose is higher than actually needed. Crossed nanotubes under low temperature irradiation (c). The amount of defects is much higher in this case since the defect annealing practically does not occur.



FIG. 6. Cross section along the axis of one of the crossed pristine nanotubes when a force of about 30 nN pushes one nanotube to the other. Although the force resulted in a substantial decrease of the intertube separation and mechanical deformation of the carbon network, welding of nanotubes does not occur even at elevated temperatures up to 2000 K.

radiation dose depends on the tube diameter. Based on our results, we predict that for SWNT's with diameters  $< 1$  nm the optimum dose ( $E_i = 0.5$ -1 keV) for welding is about  $\Phi = (0.5 - 0.7) \times 10^{15} \text{ cm}^{-2}$ , whereas for thicker nanotubes with diameters larger than 1 nm the optimum dose is  $\Phi \approx 1 \times 10^{15} \text{ cm}^{-2}$ . This irradiation dose corresponds roughly to 10 ion impacts onto the junction area.

To emphasize the importance of maintaining high temperatures during irradiation, in Fig. 5(c) we show the atomic configuration of crossed intact nanotubes after an irradiation dose of  $\Phi = 0.5 \times 10^{15} \text{ cm}^{-2}$  but at zero temperature during the irradiation. It is evident that the number of defects, especially large vacancies, is much higher than that for the case of the high-temperature irradiation considered above, since high temperatures make it possible for the defects to migrate and anneal.

In order to clarify the role of irradiation-induced defects in nanotube welding, we also simulated the behavior of crossed nanotubes at high temperatures and when a force pushes one nanotube to the other. The structure of crossed nanotubes under the applied force (to mimic attraction between a nanotube and substrate) and zero temperature has been studied by first-principle methods by Yoon *et al.*<sup>39</sup> Similar to that work, to estimate the force at a given tube separation, we slightly reduced the intertube distance and then relaxed the system while keeping the boundary atoms fixed at the nanotube ends.

We found that a force of about 30 nN results in a substantial decrease in the intertube separation and nanotube flattening near the junction area; see Fig. 6. We further found that elevating the temperature up to 2000 K in the strained sys-

tem did not break up the carbon network of these intact nanotubes, nor gave rise to formations of any bonds between the nanotubes. Thus, we conclude that welding of nanotubes is not possible without defects even if a force which presses one nanotube to the other is applied and that the reorganization of the carbon network near the junction point occurs via defect annealing and migration.

#### IV. CONCLUSIONS

We have simulated the irradiation of crossed single-walled carbon nanotubes, both suspended and deposited on substrates, with 0.4–1 keV Ar ions using empirical potential molecular dynamics. To get an insight into the behavior of irradiation-induced defects near the nanotube junction points, we also modelled the annealing of defects between ion impacts at elevated (2000 K) temperatures.

We found that ion irradiation and high temperatures can be employed for nanotube welding which is mediated by dangling bond saturation and carbon network reconstruction near the irradiation-created vacancies in the junction area. High temperatures are indispensable for these transformations, as well as for defect annealing far from the junction areas, but cannot provide nanotube welding without irradiation. We further predict that the optimum Ar ion energies are in a range of 0.4–0.6 keV, whereas the optimum irradiation doses are about  $10^{15} \text{ cm}^{-2}$ .

Thus, given that carbon nanotubes can potentially be positioned on a substrate quite accurately using an atom force microscope, ion irradiation may be used to produce a mechanically stable network of joined nanotubes with predetermined positions of junctions between nanotubes. Ion irradiation of tangled nanotubes should also give rise to formations of links between the nanotubes and an increase in the mechanical strength of the system, which might be employed in developing nanotube-based reinforcement materials.

#### ACKNOWLEDGMENTS

The research was supported by TEKES under the FFUSION2 programme, and the Academy of Finland under Projects No. 44215 and No. 73722. Grants of computer time from the Center for Scientific Computing in Espoo, Finland are gratefully acknowledged.

<sup>1</sup>A.N. Andriotis, M. Menon, D. Srivastava, and L. Chernozatonskii, Phys. Rev. B **65**, 165416 (2002).

<sup>2</sup>M. Menon and D. Srivastava, Phys. Rev. Lett. **79**, 4453 (1997).

<sup>3</sup>L. Chico, V.H. Crespi, L.X. Benedict, S.G. Louie, and M.L. Cohen, Phys. Rev. Lett. **76**, 971 (1996).

<sup>4</sup>L. Chico, M.P. López Sancho, and M.C. Muñoz, Phys. Rev. Lett. **81**, 1278 (1998).

<sup>5</sup>C.G. Rocha, T.G. Dargam, and A. Latg, Phys. Rev. B **65**, 165431 (2002).

<sup>6</sup>L. Chico, L.X. Benedict, S.G. Louie, and M.L. Cohen, Phys. Rev. B **54**, 2600 (1996).

<sup>7</sup>Z. Yao, H.W.C. Postma, L. Balents, and C. Dekker, Nature (London) **402**, 273 (1999).

<sup>8</sup>C. Papadopoulos, A. Rakitin, J. Li, A.S. Vedeneev, and J.M. Xu, Phys. Rev. Lett. **85**, 3476 (2000).

<sup>9</sup>J. Li, C. Papadopoulos, and J. Xu, Nature (London) **402**, 253 (1999).

<sup>10</sup>B.C. Satishkumar, P.J. Thomas, A. Govindaraj, and C.N.R. Rao, Appl. Phys. Lett. **77**, 2530 (2000).

<sup>11</sup>X. Ma and E.G. Wang, Appl. Phys. Lett. **78**, 978 (2001).

<sup>12</sup>J.-M. Ting and C.-C. Chang, Appl. Phys. Lett. **80**, 324 (2002).

<sup>13</sup>P. Nagy, R. Ehlich, L.P. Biró, and J. Gyulai, Appl. Phys. A: Mater.

- Sci. Process. **70**, 481 (2000).
- <sup>14</sup>P.W. Chiu, G.S. Duesberg, U. Dettlaff-Weglikowska, and S. Roth, Appl. Phys. Lett. **80**, 3811 (2002).
- <sup>15</sup>F. Banhart, Nanoletters **1**, 329 (2001).
- <sup>16</sup>B. Ni, R. Andrews, D. Jacques, D. Qian, M.B.J. Wijesundara, Y. Choi, L. Hanley, and S.B. Sinnott, Appl. Phys. A: Mater. Sci. Process. **105**, 12719 (2001).
- <sup>17</sup>M. Terrones, F. Banhart, N. Grobert, J.-C. Charlier, H. Terrones, and P. Ajayan, Phys. Rev. Lett. **89**, 075505 (2002).
- <sup>18</sup>J.-C. Charlier, T.W. Ebbesen, and P. Lambin, Phys. Rev. B **53**, 11 108 (1996).
- <sup>19</sup>L.C. Venema, J.W. Janssen, M.R. Buitelaar, J.W.G. Wildöer, S.G. Lemay, L.P. Kouwenhoven, and C. Dekker, Phys. Rev. B **62**, 5238 (2000).
- <sup>20</sup>J.W. Janssen, S.G. Lemay, L.P. Kouwenhoven, and C. Dekker, Phys. Rev. B **65**, 115423 (2002).
- <sup>21</sup>C. Thelander and L. Samuelson, Nanotechnology **13**, 108 (2002).
- <sup>22</sup>A.V. Krasheninnikov, K. Nordlund, M. Sirviö, E. Salonen, and J. Keinonen, Phys. Rev. B **63**, 245405 (2001).
- <sup>23</sup>A.V. Krasheninnikov, K. Nordlund, and J. Keinonen, Phys. Rev. B **65**, 165423 (2002).
- <sup>24</sup>K. Nordlund, J. Keinonen, and T. Mattila, Phys. Rev. Lett. **77**, 699 (1996).
- <sup>25</sup>M.P. Allen and D.J. Tildesley, *Computer Simulation of Liquids* (Oxford University Press, Oxford, England, 1989).
- <sup>26</sup>D.W. Brenner, Phys. Rev. B **42**, 9458 (1990).
- <sup>27</sup>Y. Xia, Y. Ma, Y. Xing, Y. Mu, C. Tan, and L. Me, Phys. Rev. B **61**, 11 088 (2000).
- <sup>28</sup>M.B. Nardelli, B.I. Yakobson, and J. Bernholc, Phys. Rev. B **57**, 4277 (1998).
- <sup>29</sup>K. Nordlund, N. Runeberg, and D. Sundholm, Nucl. Instr. Meth. Phys. Res. B **132**, 45 (1997).
- <sup>30</sup>J.F. Ziegler, J.P. Biersack, and U. Littmark, *The Stopping and Range of Ions in Matter* (Pergamon, New York, 1985).
- <sup>31</sup>H.J.C. Berendsen, J.P.M. Postma, W.F. van Gunsteren, A. DiNola, and J.R. Haak, J. Chem. Phys. **81**, 3684 (1984).
- <sup>32</sup>M. Terrones, H. Terrones, F. Banhart, J.-C. Charlier, and P.M. Ajayan, Science **288**, 1226 (2000).
- <sup>33</sup>F. Banhart and P.M. Ajayan, Nature (London) **382**, 433 (1996).
- <sup>34</sup>F. Banhart, Rep. Prog. Phys. **62**, 1181 (1999).
- <sup>35</sup>P.M. Ajayan, V. Ravikumar, and J.-C. Charlier, Phys. Rev. Lett. **81**, 1437 (1998).
- <sup>36</sup>Y.H. Lee, S.G. Kim, and D. Tománek, Phys. Rev. Lett. **78**, 2393 (1997).
- <sup>37</sup>A.V. Krasheninnikov, K. Nordlund, and J. Keinonen (unpublished).
- <sup>38</sup>Despite the difference in the masses of C and Ar atoms, and hence, different maximum energy transferred in a binary collision, the threshold energy for a displacement is roughly the same due to chemical interactions between carbon atoms in the nanotube.
- <sup>39</sup>Y.-G. Yoon, M.S.C. Mazzoni, H.J. Choi, J. Ihm, and S.G. Louie, Phys. Rev. Lett. **86**, 688 (2001).